HHS Public Access

Author manuscript

Arch Biochem Biophys. Author manuscript; available in PMC 2018 September 15.

Published in final edited form as:

Arch Biochem Biophys. 2017 September 15; 630: 1–8. doi:10.1016/j.abb.2017.07.009.

Association between ROS production, swelling and the respirasome integrity in cardiac mitochondria

Sehwan Jang and **Sabzali Javadov***

Department of Physiology, University of Puerto Rico School of Medicine, San Juan, Puerto Rico

Abstract

Although mitochondrial Ca^{2+} overload and ROS production play a critical role in mitochondria-mediated cell death, a cause-effect relationship between them remains elusive. This study elucidated the crosstalk between mitochondrial swelling, ROS production, and electron transfer chain (ETC) supercomplexes in rat heart mitochondria in response to Ca^{2+} and tert-butyl hydroperoxide (TBH), a lipid-soluble organic peroxide. Results showed that ROS production induced by TBH was significantly increased in the presence of Ca^{2+} in a dose-dependent manner. TBH markedly inhibited the state 3 respiration rate with no effect on the mitochondrial swelling. Ca^{2+} exerted a slight effect on mitochondrial respiration that was greatly aggravated by TBH. Analysis of supercomplexes revealed a minor difference in the presence of TBH and/or Ca^{2+}. However, incubation of mitochondria in the presence of high Ca^{2+} (1 mM) or inhibitors of ETC complexes (rotenone and antimycin A) induced disintegration of the main supercomplex, respirasome. Thus, PTP-dependent swelling of mitochondria solely depends on Ca^{2+} but not ROS. TBH has no effect on the respirasome while Ca^{2+} induces disintegration of the supercomplex only at a high concentration. Intactness of individual ETC complexes I and III is important for maintenance of the structural integrity of the respirasome.

Keywords

heart mitochondria; reactive oxygen species; calcium; ETC respirasome; mitochondrial swelling

1. Introduction

Oxidative and energetic stress during ischemia and subsequent reperfusion cause structural and functional damages to the myocardium [1]. Mechanisms contributing to the pathogenesis of ischemia-reperfusion injury are multifactorial and highly integrated. Increases in cellular Ca^{2+} and reactive oxygen species (ROS) induced by ischemia and then, amplified upon reperfusion are the main mediators of reperfusion injury [2]. Mitochondria

*Corresponding author: Sabzali Javadov, MD, PhD, Department of Physiology, School of Medicine, University of Puerto Rico, San Juan, PR 00936-5067, Tel: 787-758-2525 Ext.2909; Fax: 787-753-0120; sabzali.javadov@upr.edu.

Author Disclosure Statement: No competing financial interests exist.

have emerged as the major source of ROS as well as a critical target for cardioprotective strategies at reperfusion [3]. Mitochondrial Ca^{2+} overload accompanied by oxidative stress and increased Pi levels leads to mitochondrial permeability transition (PT) accompanied by opening non-selective PT pores (PTP) in the inner mitochondrial membrane. Sustained PTP induction stimulates mitochondria-mediated cell death through apoptosis and necrosis depending on the ATP level in the cell [4–6]. Despite intensive studies, the molecular identity of core components of the PTP complex still remains elusive, and cyclophilin D (CypD) is the only known protein that plays a key regulatory role in PTP induction [7–10]. Also, the mechanisms underlying PTP induction as well as a cause-effect relationship between Ca^{2+}-induced ROS production and PTP opening have not yet been fully understood [11].

Structural integrity of respiratory supercomplexes (SCs), large supramolecular structures of electron transfer chain (ETC) complexes, seems to be involved in the pathogenesis of mitochondrial dysfunction. Structural organization and potential role of SCs has been investigated in mitochondria and reviewed elsewhere [12]. One of the main SCs, SC I_1+III_2+IV_1, known as the respirasome, contains the ETC complexes I,III, and IV, and was found in mitochondria of rodent [13], dog [14], and bovine [15] hearts. Recently, the atomic structure of the respirasome has been resolved and potential mechanisms of SC assembling have been suggested [16–18]. According to the solid-state model, the SCs assembly can provide high-efficiency electron flux throughout the ETC, increase ATP synthesis, and reduce electron leakage and thus, mitochondrial ROS production due to short diffusion distances between individual ETC complexes [9,19–22]. However, functional and catalytic advantages of SCs are disputed, and it remains unclear whether channeling in SCs is kinetically important to provide highly efficient ATP synthesis [23]. In addition, several studies showed deterioration of SCs in various disease models [14,24–27].

Notably, cardiolipin, a signature lipid of mitochondria, is required for assembling and maintenance of the structural integrity of SCs [28,29]. Depletion of cardiolipin [30,31] and degradation of SCs [14] were found in animal models of heart failure. Loss of tafazzin, an enzyme responsible for cardiolipin remodeling, induced a 40% loss of mature cardiolipin (tetralinoleyl-cardiolipin) [32], and disintegration of SCs [25]. Degradation of SCs and oxidation of cardiolipin induced by ischemia-reperfusion in rat hearts were prevented in the presence of XJB-5-131, a mitochondria-targeted electron scavenger [25].

Thus, despite growing number of studies, the mechanism of SC degradation, particularly, the crosstalk between mitochondrial swelling, ROS generation and SC disintegration in response to oxidative and energetic stress remains to be elucidated. Our recent studies showed that ROS production and PTP-induced mitochondrial swelling can play a causative role in SC degradation in response to oxidative stress induced by ischemia-reperfusion in rat hearts [25]. In this study, we evaluated the possible relationship between mitochondrial swelling, ROS production and respirasome integrity. Our results demonstrated that although Ca^{2+} stimulates ROS production in mitochondria, swelling of mitochondria solely depends on Ca^{2+} rather than ROS. The undiminished enzymatic activity of individual ETC complexes I and III is important for maintenance of the structural integrity of SCs in cardiac mitochondria.

2. Materials and Methods

2.1 Animals

Male Sprague-Dawley rats weighing 225–275 g were purchased from Charles River (Wilmington, MA). All experiments were performed per protocols approved by the University of Puerto Rico Medical Sciences Campus Animal Care and Use Committee and conformed to the National Research Council Guide for the Care and Use of Laboratory Animals published by the U.S. National Institutes of Health (2011, Eighth Edition).

2.2 Isolation of mitochondria

Rats were deeply anesthetized with an anesthetic cocktail (179.2 mg/kg body weight, IP) containing 4.2 mg/kg xylazine, 87.5 mg/kg ketamine, and 87.5 mg/kg acepromazine to avoid any discomfort, distress, and pain in accordance with the AVMA Guidelines for the Euthanasia of Animals (2013 Edition). The depth of anesthesia was assessed by lack of response to the withdrawal reflex from a toe pinch, 15 min after the administration of anesthesia. The hearts were rapidly removed and briefly perfused by the Langendorff technique to remove blood from the tissue. Then the ventricles were homogenized with a Polytron homogenizer at 1,500 rpm for 5 sec in ice-cold sucrose buffer containing 300 mM sucrose, 10 mM Tris-HCl, and 2 mM EGTA, at pH 7.4 [33]. Mitochondria were isolated from the homogenate by centrifugation at 2,000 × g for 2 min in the sucrose buffer containing 0.5% BSA in a benchtop centrifuge to remove cell debris, followed by centrifugation of the supernatant at 10,000 × g for 5 min to sediment the mitochondrial suspension. The pellet was then washed two times at 10,000 × g for 5 min in 40 mL of sucrose buffer (BSA-free). The final pellet containing mitochondria was resuspended in 300 μL of the sucrose buffer.

2.3 Analysis of mitochondrial swelling

For analysis of mitochondrial swelling as a marker of PTP opening, freshly isolated mitochondria (0.4 mg/mL) were incubated at 37 °C in 0.1 mL of incubation buffer containing 200 mM sucrose, 10 mM Tris-MOPS, 5 mM α-ketoglutarate, 2 mM malate, 1 mM Pi, 10 μM EGTA-Tris, pH 7.4. Swelling of mitochondria was determined by monitoring the decrease in light scattering at 525 nm in the presence or absence of Ca^{2+} [33]. The absorbance was monitored for ~35 min simultaneously with or without Ca^{2+} and/or tert-butyl hydroperoxide (TBH). In additional experiments, sanglifehrin A (SfA, Novartis Pharma, Basel, Switzerland) was used to inhibit PTP opening/mitochondrial swelling.

2.4 Analysis of H_2O_2 production in mitochondria

Freshly isolated mitochondria were incubated at 37 °C in 0.1 mL of the incubation buffer containing 200 mM sucrose, 10 mM Tris-MOPS, 5 mM α-ketoglutarate, 2 mM malate, 1 mM Pi, 10 μM EGTA-Tris, pH 7.4. Production of H_2O_2 as an indicator of ROS generation was measured in isolated mitochondria with 50 μM Amplex Red (Invitrogen) in the medium containing 25 mM sodium phosphate, pH 7.4, and 0.1 U/mL HRP. Fluorescence intensity was monitored in the presence or absence of Ca^{2+} and/or TBH at an excitation of 560 nm and emission at 590 nm.

2.5 Determination of respiration rates of mitochondria

The rates of oxygen consumption were measured at 37 °C using a YSI Oxygraph (Yellow Springs, OH) model 5300 equipped with a Clark-type oxygen electrode [33]. Briefly, freshly isolated mitochondria were incubated in a buffer containing 125 mM KCl, 20 mM MOPS, 10 mM Tris, 0.5 mM EGTA, and 2 mM KH_2PO_4, at pH 7.2, supplemented with 2.5 mM 2-oxoglutarate and 1 mM L-malate to measure the rate of oxygen consumption for ETC complex I. The state 3 respiration rate was determined in the presence of 1 mM ADP. Respiration charts were recorded and analyzed using Chart5 (PowerLab) and expressed in nmols O_2 per min to mg of mitochondrial protein.

2.6 Analysis of respiratory supercomplexes

Mitochondrial SCs were analyzed by blue-native polyacrylamide gel electrophoresis (BN-PAGE) as previously described with modifications [13,24,25]. Briefly, 120 μg of mitochondrial proteins was dissolved in 100 μL of solubilization buffer (50 mM NaCl, 50 mM imidazole-HCl, 2 mM 6-aminohexanoic acid, 1 mM EDTA) supplemented with 4 μL of 20% digitonin, 1 μL protease and phosphatase inhibitor cocktails (Sigma-Aldrich), and 25 U of Benzonase®. Samples were incubated on ice for 20 min with vortex for 5 sec every 10 min and then, centrifuged for 20 min at 20,000 × g. Supernatants were collected and mixed with 30 μL of sample buffer (50 mM NaCl, 10% glycerol, 0.001% Ponceau S, 50 mM Tris-HCl, pH 7.2). BNGE was conducted as per the manufacturer's recommendations (Invitrogen). After electrophoresis, gels were stained by Coomassie brilliant blue G250 and then scanned with the Odyssey CLx Infrared Imaging System (LI-COR Biosciences) at 0.5 mm focal depth and 300 ppi (pixels per inch) resolution in high-quality mode. The resulting images were analyzed with ImageJ (NIH).

For two-dimensional blue-native SDS-PAGE (2D BN/SDS-PAGE) and immunoblotting, the lanes were cut from native gels after running and immediately incubated with loading buffer (50 mM Tris, pH 8.8, 50 mM DTT, 2% SDS, and 0.01% bromophenol blue) for 5 min. The lanes were loaded into 12% SDS-PAGE gel and sealed with 0.5% agarose. Second-dimension run and subsequent immunoblotting were conducted as per the manufacturer's recommendations (Bio-Rad). The total OXPHOS Rodent WB Antibody Cocktail (Abcam) antibodies were used for identification of ETC complexes I-V as per the manufacturer's recommendations. The signals were visualized by VersaDoc 4000 Gel Imaging System (Bio-Rad) and analyzed by ImageJ (NIH).

2.7 Statistical analysis

Data were analyzed by ANOVA with a Shapiro-Wilk test of normality and a Holm-Sidak multiple comparison test, in addition to a Student's t-test. $P < 0.05$ was considered statistically significant. Results are presented as mean ± SEM.

3. Results

3.1 Effects of Ca^{2+} and TBH on ROS production

TBH is a lipid-soluble organic peroxide, which, in comparison with H_2O_2, is more similar to endogenous lipid hydroperoxides generated during oxidative stress. Like lipid

hydroperoxides, TBH easily enters into the apolar environment in the inner mitochondrial membrane in close proximity to the hydrocarbon chains of cardiolipin. Therefore, TBH attacks and peroxidizes CL more effectively than H_2O_2 [34]. In the first set of experiments, isolated cardiac mitochondria were treated with different concentrations of TBH (0-200 μM), and H_2O_2 levels were measured by Amplex Red. The rate of H_2O_2 production was increased in the presence of TBH at a concentration of 50 μM or higher, and after 30 min, reached a 4.8-fold and 6.0-fold increase compared to the control (no TBH) for 100 and 200 μM TBH, respectively (Fig. 1A).

Next, we examined the effect of TBH on H_2O_2 production after 30 min of incubation of mitochondria in the presence of Ca^{2+} at concentrations ranging from 0 to 300 μM (Fig. 1C). The effect of Ca^{2+} was much greater than that induced by TBH alone. The rate of H_2O_2 production induced by 300 μM of Ca^{2+} alone (no TBH added) was an 8-fold greater than that induced in the absence of Ca^{2+} (0 μM). There were no significant differences between H_2O_2 production rates induced by 10 and 50 μM TBH and control (0 μM TBH) in the presence of Ca^{2+}. However, the differences induced by 100 and 200 μM TBH were statistically significant, in comparison with the control group (Fig. 1B). Importantly, the source of increased H_2O_2 was mitochondria rather than TBH as H_2O_2 produced from TBH was consumed by Amplex Red within 5-10 min, and no ROS production was observed in the absence of mitochondria (Fig. 1C and 1D).

3.2 The effects of TBH on mitochondrial respiration and swelling

In the next set of experiments, we assessed the effects of TBH on the respiration rate of mitochondria in the presence and absence of 100 μM Ca^{2+}. Results showed that 100 μM Ca^{2+} (or 250 nmoles Ca^{2+} per mg mitochondrial protein) Ca^{2+} alone (no TBH) had no significant effect on the state 3 respiration rate. Notably, TBH alone (no Ca^{2+}) at very low concentration (10 μM), which had no effect on ROS production (Fig. 1A), reduced the state 3 by 31% (P<0.05) and the effect reached the maximum value (52%, P<0.05) at 50 μM (-Ca^{2+} groups in Fig. 2). TBH at ≥50 μM had additional inhibitory effects on the respiratory function of mitochondria in the presence of 100 μM Ca^{2+}. State 3 was reduced by 32, 53 and 38% (P<0.01 for all) in the presence of 50, 100 and 200 μM TBH, respectively.

Analysis of mitochondrial absorbance data revealed no significant effect of TBH on the swelling in both the presence and absence of Ca^{2+} (Fig. 3). Rates of basal (no Ca^{2+} added) and Ca^{2+}-induced swelling were not affected by TBH at all concentrations. Thus, these data demonstrate that, in the absence of Ca^{2+}, TBH-induced ROS has an inhibitory effect on mitochondrial respiration, but not swelling.

3.3 Inhibition of CypD on H_2O_2 production

Next, we analyzed the effect of CypD inhibition on H_2O_2 production. As shown in Figure 4A, swelling of cardiac mitochondria was initiated by addition of 175 μM Ca^{2+} (438 nmoles Ca^{2+} per mg mitochondrial protein). Sanglifehrin A (SfA), a CypD inhibitor, attenuated the mitochondrial swelling by enhancing the tolerance to Ca^{2+} (or resistance to PTP opening) by 29%. Mitochondrial swelling in the presence of SfA started at 225 μM Ca^{2+} (Fig. 4A).

The similar effect was observed with H_2O_2 production induced by 175 and 200 μM Ca^{2+}. Pretreatment of mitochondria with SfA reduced the rate of H_2O_2 production by 46% and 36% ($P<0.05$ for both) induced by 175 and 200 μM Ca^{2+}, respectively (Fig. 4B). However, SfA was not able to inhibit the ROS production induced by high concentrations (≥ 225 μM) of Ca^{2+}. Notably, SfA *per se* had no any antioxidant capacity in the absence of mitochondria (Fig. S1). These data suggest that the effect of SfA to attenuate ROS production is secondary to inhibition of the PTP.

3.4 The effects of TBH and Ca^{2+} on the integrity of SCs

In the next set of experiments, we analyzed respiratory SCs in cardiac mitochondria pretreated with TBH and Ca^{2+}. Each band after BN-PAGE was identified by 2D SDS-PAGE (Fig. 5A and S3). Analysis of histogram revealed that brightest band at ~850 kDa (peak 5 in Fig. 5B), which was designated as respiratory complex V dimers [25], also contains peaks from other complexes. Furthermore, the peak 7 known as a respiratory complex I monomer, also contains peaks from ETC complexes II (traces), III, and IV. Two faint bands at 1048 kDa and 1236 kDa (peaks 1 and 3, respectively) were also correlated with peaks from complex V known as complex V tetramers and hexamers [35].

We performed BN-PAGE analysis of mitochondria pretreated with TBH and Ca^{2+} at different concentrations. Results demonstrated that TBH or Ca^{2+} induces minor changes in respirasome levels (*data not shown*). However, the respirasome was reduced by 16.1% ($P<0.05$) in mitochondria treated with Ca^{2+} at very high concentration (1 mM Ca^{2+} or 2.5 μmoles Ca^{2+} per mg mitochondrial protein) (Fig. 5C-E). In addition, we analyzed potential effects of inhibition of the ETC complexes I and III on the integrity of SCs. The complexes I and III are involved in the respirasome (SC I_1+III_2+IV_1), the main SC, that apparently plays an important role in the ETC activity. Interestingly, we revealed noticeable changes in SCs in mitochondria treated with 2 μM rotenone (complex I inhibitor) and 1 μM antimycin A (complex III inhibitor), which induced a 20.1% ($P<0.01$) and 13.0% ($P<0.01$) reductions of SCs, respectively, compared to untreated (control) mitochondria (Fig. 5C-E, (peaks 1~4)). These data demonstrate that TBH has little effect on SCs however Ca^{2+} at very high concentration (1 mM) and inhibition of ETC complexes I and III stimulate degradation of SCs, particularly, the respirasome.

It should be noted that, we analyzed SCs also by 2D BN/SDS-PAGE and immunoblotting. Results of these studies are presented in Fig. S3. Quantification of immunoblots after 2D BN/SDS-PAGE did not provide statistically significant differences between control and treated mitochondria. Similar observations have been reported in our previous study [25]. So we preferably used results obtained by BN-PAGE for comparison of experimental groups.

4. Discussion

Reperfusion after sustained ischemia causes Ca^{2+} overload, ROS production, and PTP induction in mitochondria; however, a cause-effect relationship between these events has not been fully understood [11]. Furthermore, the role of respiratory SCs in physiology and pathophysiology of cardiac mitochondria still remains elusive. Our study demonstrated that: (i) Ca^{2+} and/or ROS stimulates ROS production in mitochondria and, ROS, but not Ca^{2+}

inhibit respiratory function of mitochondria, (ii) ROS alone do not stimulate PTP induction, (iii) inhibition of CypD, a major PTP regulator, increases the Ca^{2+} tolerance; it delays mitochondrial swelling (PTP opening) and attenuates ROS production within the tolerance range, and (iv) Ca^{2+} or ROS causes minor changes in respiratory SCs, however inhibition of ETC complexes I or III disintegrates SCs, particularly, the respirasome.

Mitochondrial ETC complexes are able to be dynamically assembled into SCs, although the functional role of SCs is not clear. Degradation of SCs significantly increases ROS production at complex I suggesting that SCs prevents excessive ROS generation [36]. It was suggested that SCs can regulate the electron flux from different substrates through the respiratory chain [21], however a robust flux control analysis provided no evidence for substrate channeling between the ETC complexes assembled in SCs [23]. In addition, although the structural identity of SCs has been extensively investigated [16–18,37], the contribution of SCs to mitochondrial dysfunction and mitochondria-mediated cell death remains unclear. In our previous studies, we observed a 40% reduction of respirasome in cardiac mitochondria isolated from tafazzin knock-down mice, in contrast to a 3% decrease of the respirasome after ischemia (25 min) and reperfusion (60 min) in rat hearts [25]. It should be noted, the impact of a small reduction of SC levels on mitochondrial function during ischemia-reperfusion is not clear. Although the hearts had low post-ischemic recovery (23% of pre-ischemia), enzymatic activity of ETC complexes, except complex III, were not affected by cardiac ischemia-reperfusion [25]. These data suggest that: 1) early dysfunction of mitochondrial respirasome may be beyond of the changes in its quantity, and associated with the activity of ETC individual complexes, and 2) quantification of SCs BN-PAGE technique may not accurately/precisely estimate the actual changes in SC levels which can be effected by isolation, solubilization, electrophoresis, staining and other procedures during analysis. Results of the present study demonstrated that inhibition of ETC complexes I or III triggered degradation of SCs in isolated mitochondria. These data suggest that SC assembling and integrity is dependent on the enzymatic activity of individual ETC complexes. Notably, growing number of studies demonstrate interdependence between ETC individual complexes involved in SCs (*Reviewed in* [38,39]). Deficiencies in expression of complexes III [40] and IV [41] was associated with a reduction of complex I levels. On the other hand, disruption of complex I by NDUFS4 mutations diminished complex III activity in human skin fibroblasts [42]. These studies provide strong evidence that unaltered activity and molecular integrity of individual complexes I, III and IV is required for SCs, particularly, the respirasome assembly. Although complex II is not involved in respirasome structure [43], and represents the only rate-limiting step in succinate oxidation, it can play a role in maintenance of the respirasome SCs indirectly. For example, complex II is tightly coupled to complexes I and III, and has been recognized as a source of ROS generation [44,45]. Accordingly, changes in complex II activity can stimulate ROS production and thus, induce SC disorganization through oxidation of cardiolipin. New studies are required to clarify the contribution of all ETC complexes to SC assembling. Our studies do not exclude non-specific effects of rotenone and antimycin A to induce conformational changes in the structure of SC molecules leading to their disintegration.

Our results demonstrated that Ca^{2+} alone induces H_2O_2 production (Fig.1B), which was concomitant with PTP-dependent swelling of mitochondria (Fig. 4A). Pretreatment of

mitochondria with SfA reduced ROS production indicating at PTP-induced ROS production (Fig. 4B). The cause-effect relationship between ROS and PTP induction has not yet been fully established. Similar to our findings, several studies reported that Ca^{2+}-induced PTP opening stimulates ROS production [46,47]. On the other hand, ROS can modulate mitochondrial redox environment through CypD oxidation. Hydrogen peroxide affected conformation and enzymatic activity of CypD and thereby, stimulated PTP opening [48,49]. Changes in redox state of CypD due to its oxidation can modulate activity of other PTP regulators such as ANT, P_iC, and F_0F_1-ATP synthase, and induce pore opening. In our studies, TBH alone did not induce mitochondrial swelling whereas Ca^{2+} alone significantly stimulated the swelling which was further increased in the presence of TBH. These data are consistent with previous findings that demonstrated no osmotic alteration induced by 100 μM TBH in rat heart mitochondria [50]. This study also found no effect of 30 μM Ca^{2+} alone to induce swelling in mitochondria (0.5 mg/ml) that can be explained with low concentration of the ion. Our present (Fig. 3B) and previous studies [25] showed that Ca^{2+} at concentrations up to 175 μM does not induce notable PTP opening in mitochondria (0.4 mg/ml). In contrast to our findings obtained on isolated mitochondria, ROS-induced PTP induction was observed in cultured cardiomyocytes [51] could include many other non-mitochondrial factors.

We showed that inhibition of CypD with SfA increases the Ca^{2+} tolerance of the mitochondria to initiate the massive swelling by ~30% (Fig.4A), in addition to the attenuation of ROS production within the increased tolerance range. These data suggest that, in fact, the inhibition of CypD only delays PTP opening by increasing the threshold but does not reduce the extent of PTP opening. In addition, the inhibitory effect of SfA occurs at certain concentrations of Ca^{2+} ranging from 100 to 300 μM, and mitochondrial swelling induced by Ca^{2+} above the threshold is not inhibited by SfA. In favor of this, we have previously observed that lactate dehydrogenase release (an indicator of cell death) from rat hearts was attenuated by SfA treatment only at 30 min of reperfusion and no significant differences were found at 50 min of reperfusion [25]. This observation can explain recent negative results from clinical trials [52,53] that showed no cardioprotective effects of cyclosporine A, a classic inhibitor of CypD, in patients with STEMI (ST-Elevation Myocardial Infarction). Unlike experimental studies where the threshold for PTP opening can be regulated, the effect of the insult on mitochondria (Ca^{2+} levels) may be above the threshold in the clinical setting. Also, the timing of administration of PTP inhibitors may affect clinical outcomes because PTP opening occurs during the first minutes of reperfusion [54,55].

It should be noted that TBH greatly inhibited the state 3 respiration rate concomitant with stimulation of ROS production. Since mitochondrial function depends on the redox state, it is important to elucidate how redox signals modulate mitochondrial metabolism and function [56]. Therefore, inhibition of ROS production at complexes I and III as well as scavenging of mitochondrial ROS are important for prevention mitochondria-mediated cell death. Indeed, suppressors of ROS production at Q site of the ETC complex I protected against ischemia-reperfusion injury [57]. Furthermore, in addition to the inhibition of CypD [25], scavenging of mitochondrial ROS improved post-ischemic recovery of the Langendorff-perfused rat heart [58]. We observed a 60% inhibition of state 3 respiration rate

in mitochondria of the rat heart underwent ischemia-reperfusion [25] and the extent of the inhibition is similar to that obtained with TBH and Ca^{2+} in this study. Although our study showed the role of Ca^{2+} in ROS production, further studies are required for an understanding of the mechanisms underlying the cross-talk between Ca^{2+} homeostasis and ROS production in mitochondria.

5. Conclusion

This study shows that although ROS can solely stimulate ROS production, Ca^{2+} apparently is a leading factor in mitochondrial ROS production in isolated cardiac mitochondria. ROS have no direct effect on basal and Ca^{2+}-induced swelling in isolated mitochondria thus suggesting that Ca^{2+} but not ROS plays a leading role in PTP induction. Respiratory SCs demonstrate minor differences in response to increased mitochondrial ROS and swelling implying that disintegration of SCs is the consequence rather than the cause of mitochondrial dysfunction. Inhibition of the ETC complexes I or III induces disintegration of the respirasome implying that intact (unaltered) activity of the complexes is required for maintenance of the structural integrity of SCs.

Supplementary Material

Refer to Web version on PubMed Central for supplementary material.

Acknowledgments

This study was supported by the NHLBI NIH Grants SC1HL118669 (to S.J.) and in part, by the National Center for Research Resources NIH Grants G12RR-003051 and G12MD007600.

References

1. Ibáñez B, Heusch G, Ovize M, Van de Werf F. Evolving therapies for myocardial ischemia/reperfusion injury. J Am Coll Cardiol. 2015; 65:1454–1471. DOI: 10.1016/j.jacc.2015.02.032 [PubMed: 25857912]
2. Lejay A, Fang F, John R, Van JAD, Barr M, Thaveau F, Chakfe N, Geny B, Scholey JW. Ischemia reperfusion injury, ischemic conditioning and diabetes mellitus. J Mol Cell Cardiol. 2016; 91:11–22. DOI: 10.1016/j.yjmcc.2015.12.020 [PubMed: 26718721]
3. Muntean DM, Sturza A, Dănilă MD, Borza C, Duicu OM, Mornoș C. The role of mitochondrial reactive oxygen species in cardiovascular injury and protective strategies. Oxid Med Cell Longev. 2016; 2016:8254942.doi: 10.1155/2016/8254942 [PubMed: 27200148]
4. Crompton M. The mitochondrial permeability transition pore and its role in cell death. Biochem J. 1999; 341:233–249. DOI: 10.1042/bj3410233 [PubMed: 10393078]
5. Halestrap AP, Kerr PM, Javadov S, Woodfield KY. Elucidating the molecular mechanism of the permeability transition pore and its role in reperfusion injury of the heart. Biochim Biophys Acta. 1998; 1366:79–94. [PubMed: 9714750]
6. Halestrap AP, Clarke SJ, Javadov SA. Mitochondrial permeability transition pore opening during myocardial reperfusion—a target for cardioprotection. Cardiovasc Res. 2004; 61:372–385. [PubMed: 14962470]
7. Elrod JW, Wong R, Mishra S, Vagnozzi RJ, Sakthievel B, Goonasekera SA, Karch J, Gabel S, Farber J, Force T, Brown JH, Murphy E, Molkentin JD. Cyclophilin D controls mitochondrial pore–dependent Ca^{2+} exchange, metabolic flexibility, and propensity for heart failure in mice. J Clin Invest. 2010; 120:3680–3687. DOI: 10.1172/JCI43171 [PubMed: 20890047]

8. Gutiérrez-Aguilar M, Baines CP. Structural mechanisms of cyclophilin D-dependent control of the mitochondrial permeability transition pore. Biochim Biophys Acta. 2015; 1850:2041–2047. DOI: 10.1016/j.bbagen.2014.11.009 [PubMed: 25445707]
9. Chaban Y, Boekema EJ, Dudkina NV. Structures of mitochondrial oxidative phosphorylation supercomplexes and mechanisms for their stabilisation. Biochim Biophys Acta BBA-Bioenerg. 2014; 1837:418–426.
10. Javadov S, Kuznetsov A. Mitochondrial permeability transition and cell death: the role of cyclophilin d. Front Physiol. 2013; 4:76.doi: 10.3389/fphys.2013.00076 [PubMed: 23596421]
11. Adam-Vizi V, Starkov AA. Calcium and mitochondrial reactive oxygen species generation: How to read the facts. J Alzheimers Dis JAD. 2010; 20:S413–S426. DOI: 10.3233/JAD-2010-100465 [PubMed: 20421693]
12. Guo R, Gu J, Wu M, Yang M. Amazing structure of respirasome: unveiling the secrets of cell respiration. Protein Cell. 2016; :1–12. DOI: 10.1007/s13238-016-0329-7 [PubMed: 26687327]
13. Wittig I, Carrozzo R, Santorelli FM, Schägger H. Supercomplexes and subcomplexes of mitochondrial oxidative phosphorylation. Biochim Biophys Acta BBA-Bioenerg. 2006; 1757:1066–1072.
14. Rosca MG, Vazquez EJ, Kerner J, Parland W, Chandler MP, Stanley W, Sabbah HN, Hoppel CL. Cardiac mitochondria in heart failure: decrease in respirasomes and oxidative phosphorylation. Cardiovasc Res. 2008; 80:30–39. [PubMed: 18710878]
15. Schägger H, Pfeiffer K. Supercomplexes in the respiratory chains of yeast and mammalian mitochondria. EMBO J. 2000; 19:1777–1783. [PubMed: 10775262]
16. Letts JA, Fiedorczuk K, Sazanov LA. The architecture of respiratory supercomplexes. Nature. 2016; 537:644–648. [PubMed: 27654913]
17. Gu J, Wu M, Guo R, Yan K, Lei J, Gao N, Yang M. The architecture of the mammalian respirasome. Nature. 2016
18. Sousa JS, Mills DJ, Vonck J, Kühlbrandt W. Functional asymmetry and electron flow in the bovine respirasome. eLife. 2016; 5:e21290.doi: 10.7554/eLife.21290 [PubMed: 27830641]
19. Acín-Pérez R, Fernández-Silva P, Peleato ML, Pérez-Martos A, Enriquez JA. Respiratory active mitochondrial supercomplexes. Mol Cell. 2008; 32:529–539. [PubMed: 19026783]
20. Bianchi C, Genova ML, Castelli GP, Lenaz G. The mitochondrial respiratory chain is partially organized in a supercomplex assembly kinetic evidence using flux control analysis. J Biol Chem. 2004; 279:36562–36569. [PubMed: 15205457]
21. Lapuente-Brun E, Moreno-Loshuertos R, Acín-Pérez R, Latorre-Pellicer A, Colás C, Balsa E, Perales-Clemente E, Quirós PM, Calvo E, Rodríguez-Hernández MA, et al. Supercomplex assembly determines electron flux in the mitochondrial electron transport chain. Science. 2013; 340:1567–1570. [PubMed: 23812712]
22. Lopez-Fabuel I, Douce JL, Logan A, James AM, Bonvento G, Murphy MP, Almeida A, Bolaños JP. Complex I assembly into supercomplexes determines differential mitochondrial ROS production in neurons and astrocytes. Proc Natl Acad Sci. 2016; 113:13063–13068. DOI: 10.1073/pnas.1613701113 [PubMed: 27799543]
23. Blaza JN, Serreli R, Jones AJ, Mohammed K, Hirst J. Kinetic evidence against partitioning of the ubiquinone pool and the catalytic relevance of respiratory-chain supercomplexes. Proc Natl Acad Sci. 2014; 111:15735–15740. [PubMed: 25331896]
24. Gómez LA, Monette JS, Chavez JD, Maier CS, Hagen TM. Supercomplexes of the mitochondrial electron transport chain decline in the aging rat heart. Arch Biochem Biophys. 2009; 490:30–35. [PubMed: 19679098]
25. Jang S, Lewis TS, Powers C, Khuchua Z, Baines CP, Wipf P, Javadov S. Elucidating mitochondrial electron transport chain supercomplexes in the heart during ischemia– reperfusion. Antioxid Redox Signal. 2016; doi: 10.1089/ars.2016.6635
26. Antoun G, McMurray F, Thrush AB, Patten DA, Peixoto AC, Slack RS, McPherson R, Dent R, Harper ME. Impaired mitochondrial oxidative phosphorylation and supercomplex assembly in rectus abdominis muscle of diabetic obese individuals. Diabetologia. 2015; 58:2861–2866. DOI: 10.1007/s00125-015-3772-8 [PubMed: 26404066]

27. Javadov S, Jang S, Rodriguez-Reyes N, Rodriguez-Zayas AE, Hernandez JS, Krainz T, Wipf P, Frontera W. Mitochondria-targeted antioxidant preserves contractile properties and mitochondrial function of skeletal muscle in aged rats. Oncotarget. 2015; 6:39469–39481. [PubMed: 26415224]
28. Zhang M, Mileykovskaya E, Dowhan W. Gluing the respiratory chain together: Cardiolipin is required for supercomplex formation in the inner mitochondrial membrane. J Biol Chem. 2002; 277:43553–43556. [PubMed: 12364341]
29. Zhang M, Mileykovskaya E, Dowhan W. Cardiolipin is essential for organization of complexes III and IV into a supercomplex in intact yeast mitochondria. J Biol Chem. 2005; 280:29403–29408. [PubMed: 15972817]
30. Sparagna GC, Chicco AJ, Murphy RC, Bristow MR, Johnson CA, Rees ML, Maxey ML, McCune SA, Moore RL. Loss of cardiac tetralinoleoyl cardiolipin in human and experimental heart failure. J Lipid Res. 2007; 48:1559–1570. [PubMed: 17426348]
31. Lesnefsky EJ, Slabe TJ, Stoll MS, Minkler PE, Hoppel CL. Myocardial ischemia selectively depletes cardiolipin in rabbit heart subsarcolemmal mitochondria. Am J Physiol Heart Circ Physiol. 2001; 280:H2770–2778. [PubMed: 11356635]
32. Szczepanek K, Allegood J, Aluri H, Hu Y, Chen Q, Lesnefsky EJ. Acquired deficiency of tafazzin in the adult heart: Impact on mitochondrial function and response to cardiac injury. Biochim Biophys Acta BBA - Mol Cell Biol Lipids. 2016; 1861:294–300. DOI: 10.1016/j.bbalip.2015.12.004
33. Jang S, Javadov S. Inhibition of JNK aggravates the recovery of rat hearts after global ischemia: the role of mitochondrial JNK. PloS One. 2014; 9:e113526. [PubMed: 25423094]
34. Musatov A. Contribution of peroxidized cardiolipin to inactivation of bovine heart cytochrome c oxidase. Free Radic Biol Med. 2006; 41:238–246. DOI: 10.1016/j.freeradbiomed.2006.03.018 [PubMed: 16814104]
35. Wittig I, Schägger H. Structural organization of mitochondrial ATP synthase. Biochim Biophys Acta BBA - Bioenerg. 2008; 1777:592–598. DOI: 10.1016/j.bbabio.2008.04.027
36. Maranzana E, Barbero G, Falasca AI, Lenaz G, Genova ML. Mitochondrial respiratory supercomplex association limits production of reactive oxygen species from complex I. Antioxid Redox Signal. 2013; 19:1469–1480. [PubMed: 23581604]
37. Kühlbrandt W. Structure and function of mitochondrial membrane protein complexes. BMC Biol. 2015; 13:1. [PubMed: 25555396]
38. Acin-Perez R, Enriquez JA. The function of the respiratory supercomplexes: the plasticity model. Biochim Biophys Acta BBA-Bioenerg. 2014; 1837:444–450.
39. Genova ML, Lenaz G. Functional role of mitochondrial respiratory supercomplexes. Biochim Biophys Acta BBA-Bioenerg. 2014; 1837:427–443.
40. Acín-Pérez R, Bayona-Bafaluy MP, Fernández-Silva P, Moreno-Loshuertos R, Pérez-Martos A, Bruno C, Moraes CT, Enrĺquez JA. Respiratory complex III is required to maintain complex I in mammalian mitochondria. Mol Cell. 2004; 13:805–815. [PubMed: 15053874]
41. D'Aurelio M, Gajewski CD, Lenaz G, Manfredi G. Respiratory chain supercomplexes set the threshold for respiration defects in human mtDNA mutant cybrids. Hum Mol Genet. 2006; 15:2157–2169. [PubMed: 16740593]
42. Scacco S, Petruzzella V, Budde S, Vergari R, Tamborra R, Panelli D, van den Heuvel LP, Smeitink JA, Papa S. Pathological mutations of the human NDUFS4 gene of the 18-kDa (AQDQ) subunit of complex I affect the expression of the protein and the assembly and function of the complex. J Biol Chem. 2003; 278:44161–44167. [PubMed: 12944388]
43. Schägger H, Pfeiffer K. The ratio of oxidative phosphorylation complexes I–V in bovine heart mitochondria and the composition of respiratory chain supercomplexes. J Biol Chem. 2001; 276:37861–37867. [PubMed: 11483615]
44. Siebels I, Dröse S. Q-site inhibitor induced ROS production of mitochondrial complex II is attenuated by TCA cycle dicarboxylates. Biochim Biophys Acta BBA-Bioenerg. 2013; 1827:1156–1164.
45. Chouchani ET, Methner C, Nadtochiy SM, Logan A, Pell VR, Ding S, James AM, Cochemé HM, Reinhold J, Lilley KS, et al. Cardioprotection by S-nitrosation of a cysteine switch on mitochondrial complex I. Nat Med. 2013; 19:753. [PubMed: 23708290]

46. Batandier C, Leverve X, Fontaine E. Opening of the mitochondrial permeability transition pore induces reactive oxygen species production at the level of the respiratory chain complex I. J Biol Chem. 2004; 279:17197–17204. DOI: 10.1074/jbc.M310329200 [PubMed: 14963044]

47. Kim JS, Wang JH, Lemasters JJ. Mitochondrial permeability transition in rat hepatocytes after anoxia/reoxygenation: role of Ca2+-dependent mitochondrial formation of reactive oxygen species. Am J Physiol - Gastrointest Liver Physiol. 2012; 302:G723–G731. DOI: 10.1152/ajpgi.00082.2011 [PubMed: 22241863]

48. Linard D, Kandlbinder A, Degand H, Morsomme P, Dietz KJ, Knoops B. Redox characterization of human cyclophilin D: identification of a new mammalian mitochondrial redox sensor? Arch Biochem Biophys. 2009; 491:39–45. [PubMed: 19735641]

49. Folda A, Citta A, Scalcon V, Calì T, Zonta F, Scutari G, Bindoli A, Rigobello MP. Mitochondrial thioredoxin system as a modulator of cyclophilin D redox state. Sci Rep. 2016; 6

50. Petrosillo G, Moro N, Ruggiero FM, Paradies G. Melatonin inhibits cardiolipin peroxidation in mitochondria and prevents the mitochondrial permeability transition and cytochrome c release. Free Radic Biol Med. 2009; 47:969–974. [PubMed: 19577639]

51. Zorov DB, Filburn CR, Klotz LO, Zweier JL, Sollott SJ. Reactive oxygen species (ROS)-induced ROS release: a new phenomenon accompanying induction of the mitochondrial permeability transition in cardiac myocytes. J Exp Med. 2000; 192:1001–1014. [PubMed: 11015441]

52. Cung TT, Morel O, Cayla G, Rioufol G, Garcia-Dorado D, Angoulvant D, Bonnefoy-Cudraz E, Guérin P, Elbaz M, Delarche N, et al. Cyclosporine before PCI in patients with acute myocardial infarction. N Engl J Med. 2015; 373:1021–1031. [PubMed: 26321103]

53. Trankle C, Thurber CJ, Toldo S, Abbate A. Mitochondrial membrane permeability inhibitors in acute myocardial infarction: still awaiting translation. JACC Basic Transl Sci. 2016; 1:524–535. DOI: 10.1016/j.jacbts.2016.06.012

54. Domañska-Janik K, Bużañska L, D\lużniewska J, Koz\lowska H, Sarnowska A, Zab\locka B. Neuroprotection by cyclosporin A following transient brain ischemia correlates with the inhibition of the early efflux of cytochrome C to cytoplasm. Mol Brain Res. 2004; 121:50–59. [PubMed: 14969736]

55. Hausenloy DJ, Duchen MR, Yellon DM. Inhibiting mitochondrial permeability transition pore opening at reperfusion protects against ischaemia–reperfusion injury. Cardiovasc Res. 2003; 60:617–625. DOI: 10.1016/j.cardiores.2003.09.025 [PubMed: 14659807]

56. Mailloux RJ, Jin X, Willmore WG. Redox regulation of mitochondrial function with emphasis on cysteine oxidation reactions. Redox Biol. 2013; 2:123–139. DOI: 10.1016/j.redox.2013.12.011 [PubMed: 24455476]

57. Brand MD, Goncalves RL, Orr AL, Vargas L, Gerencser AA, Jensen MB, Wang YT, Melov S, Turk CN, Matzen JT, et al. Suppressors of superoxide-H2O2 production at site I Q of mitochondrial complex I protect against stem cell yyperplasia and ischemia-reperfusion injury. Cell Metab. 2016; 24:582–592. [PubMed: 27667666]

58. Escobales N, Nuñez RE, Jang S, Parodi-Rullan R, Ayala-Peña S, Sacher JR, Skoda EM, Wipf P, Frontera W, Javadov S. Mitochondria-targeted ROS scavenger improves post-ischemic recovery of cardiac function and attenuates mitochondrial abnormalities in aged rats. J Mol Cell Cardiol. 2014; 77:136–146. [PubMed: 25451170]

Abbreviations Used

BN-PAGE	blue native polyacrylamide gel electrophoresis
CypD	cyclophilin D
2D BN/SDS-PAGE	two-dimensial blue native SDS-PAGE
ETC	electron transfer chain
PTP	permeability transition pore

ROS	reactive oxygen species
SC	supercomplex
SDS	sodium dodecyl sulfate
SfA	sanglifehrin A
TBH	tert-butyl hydroperoxide

Highlights

1. PTP-dependent swelling of mitochondria solely depends on Ca^{2+} but not ROS.
2. TBH significantly inhibits respiration of mitochondria.
3. TBH has no effect on the respirasome assembly.
4. Ca^{2+} only at a high concentration induces respirasome dissembling.
5. Integrity of respirasome depends on the activity of ETC complexes I and III.

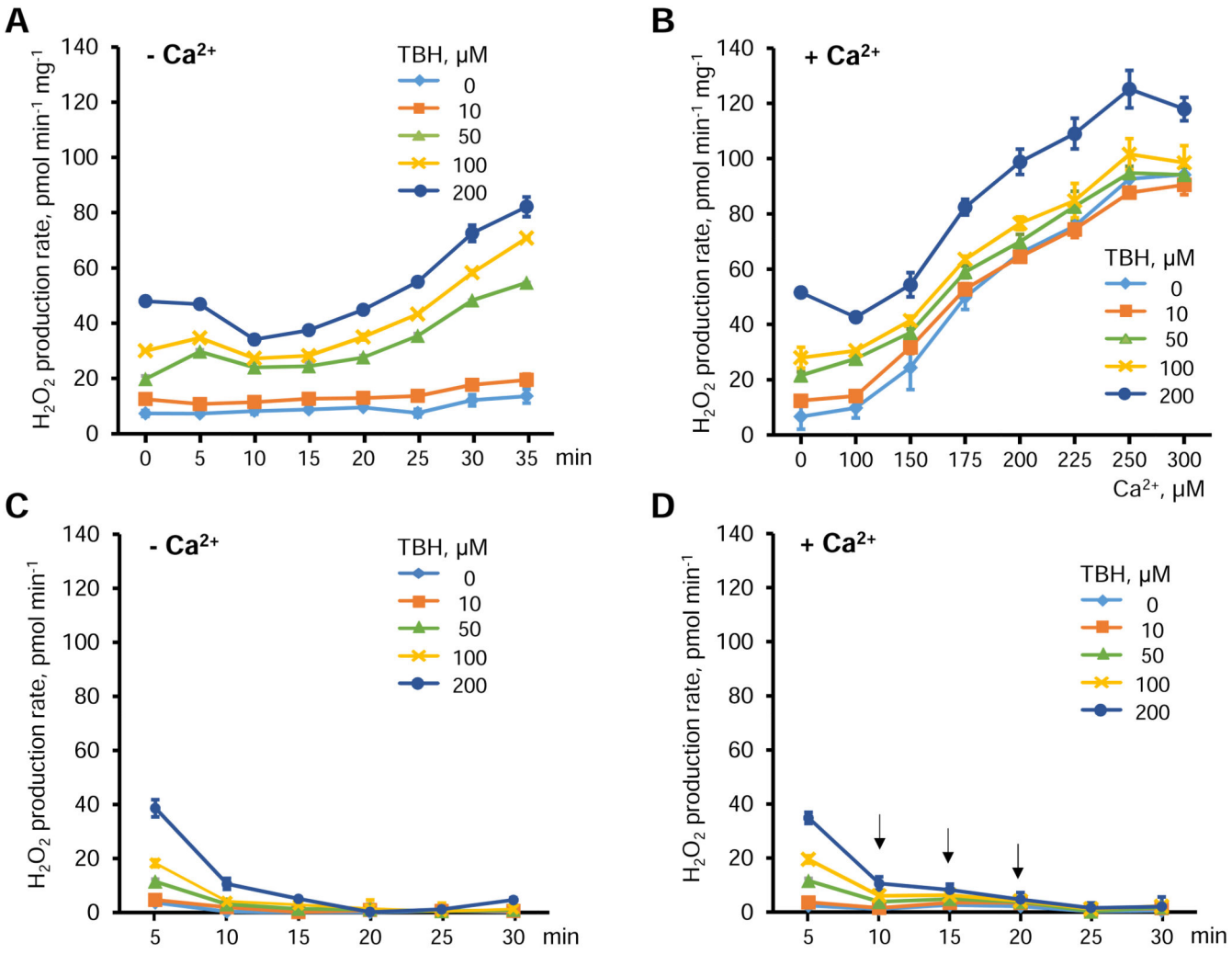

Figure 1.

The effects of TBH and Ca^{2+} on the H_2O_2 production rate in isolated mitochondria. ***A,*** Time-dependent changes of H_2O_2 production rates induced by TBH in the concentration range of 0-200 μM. ***B***, Rates of H_2O_2 production induced by Ca^{2+} (0-300 μM) and TBH (0-200 μM). ***C,D,*** Effects of TBH on H_2O_2 production in the absence ***(C)*** and presence ***(D)*** of Ca^{2+} in mitochondria-free buffer. Each arrow in ***D*** indicates the addition of 100 μM Ca^{2+}. Data are shown as means ± SEM (n=6).

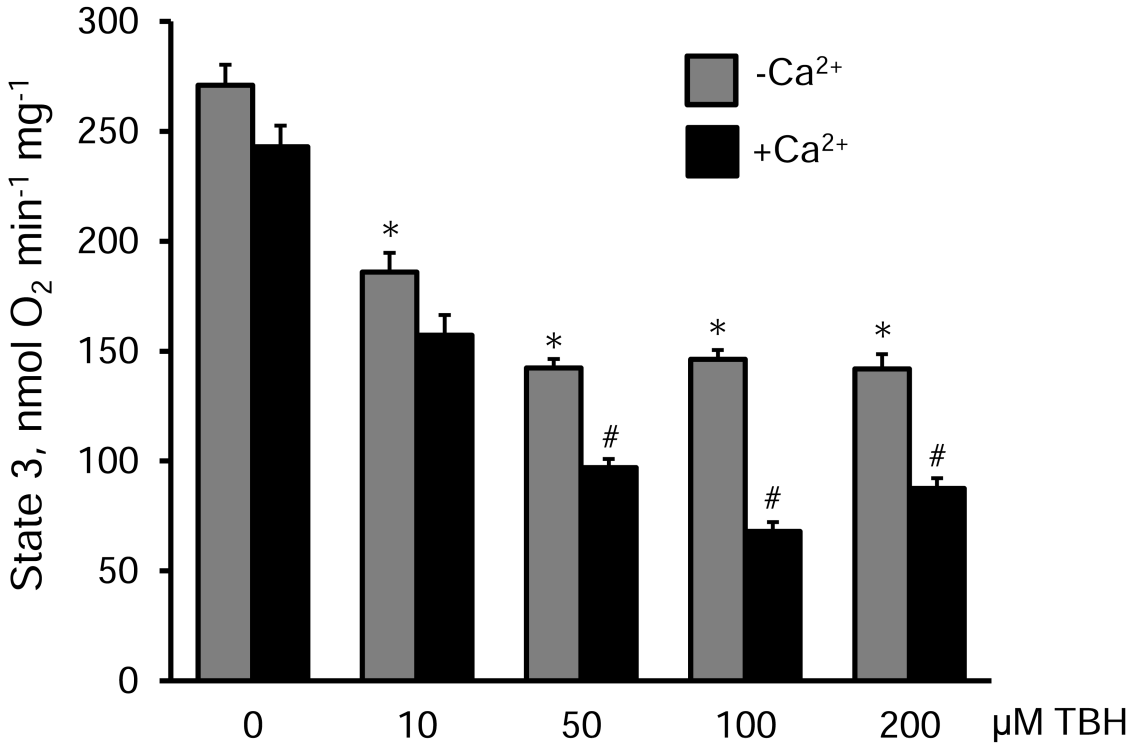

Figure 2.

The effects of TBH on the state 3 respiration rate of mitochondria in the presence or absence of 100 μM Ca^{2+}. The respiration rate is given in nmols of consumed O_2 per min per milligram of mitochondrial protein. * $P<0.05$ vs. control (no TBH); $^{\#}P<0.01$, $+Ca^{2+}$ group vs. $-Ca^{2+}$ group. Data are shown as means ± SEM (n=3).

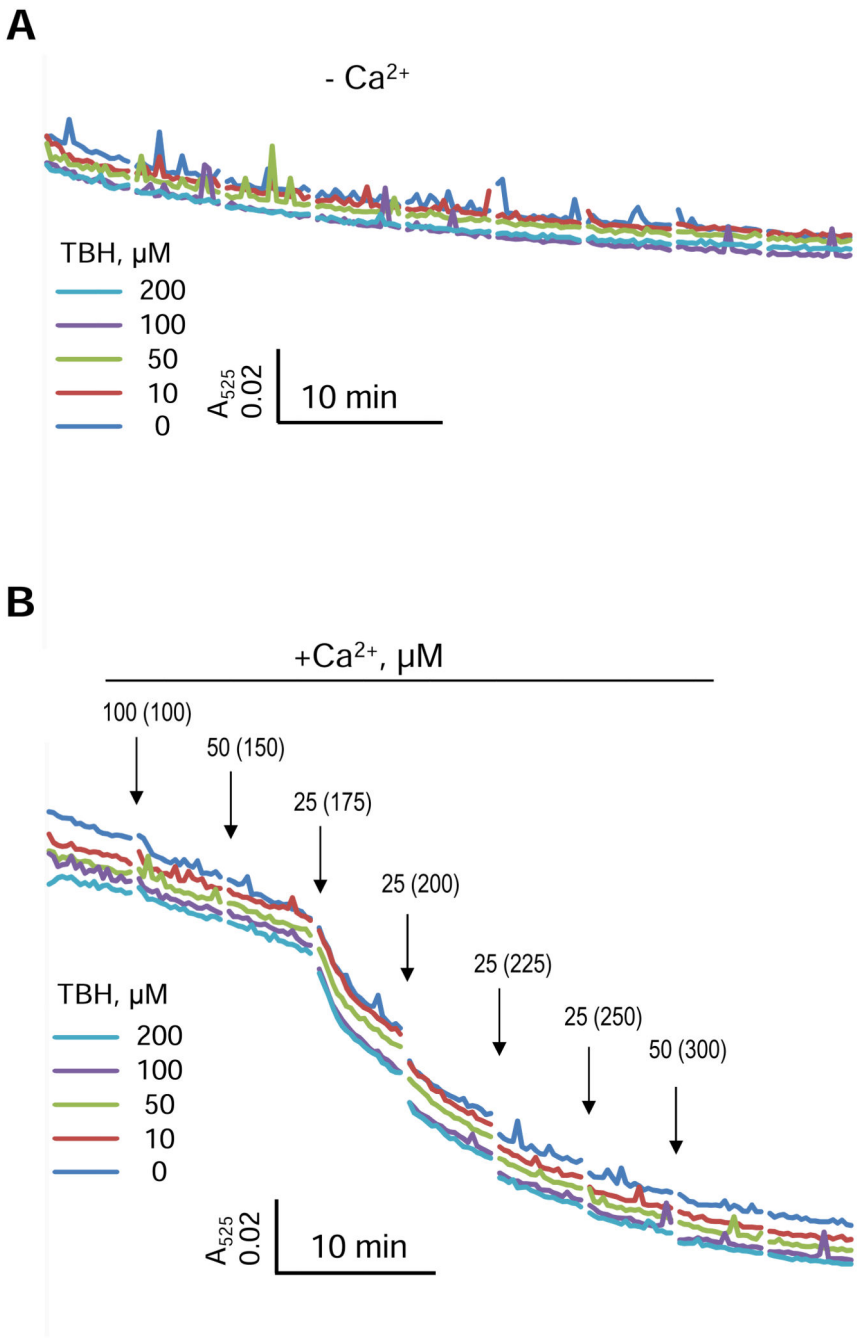

Figure 3.

Swelling of isolated mitochondria induced by TBH in the concentration range of 0-200 μM without (***A***) or with (***B***) addition of Ca^{2+}. Each arrow indicates the addition of Ca^{2+} and final concentrations of Ca^{2+} for each point are given in brackets. The representative curves with error bars are shown in Supplementary Figure S2.

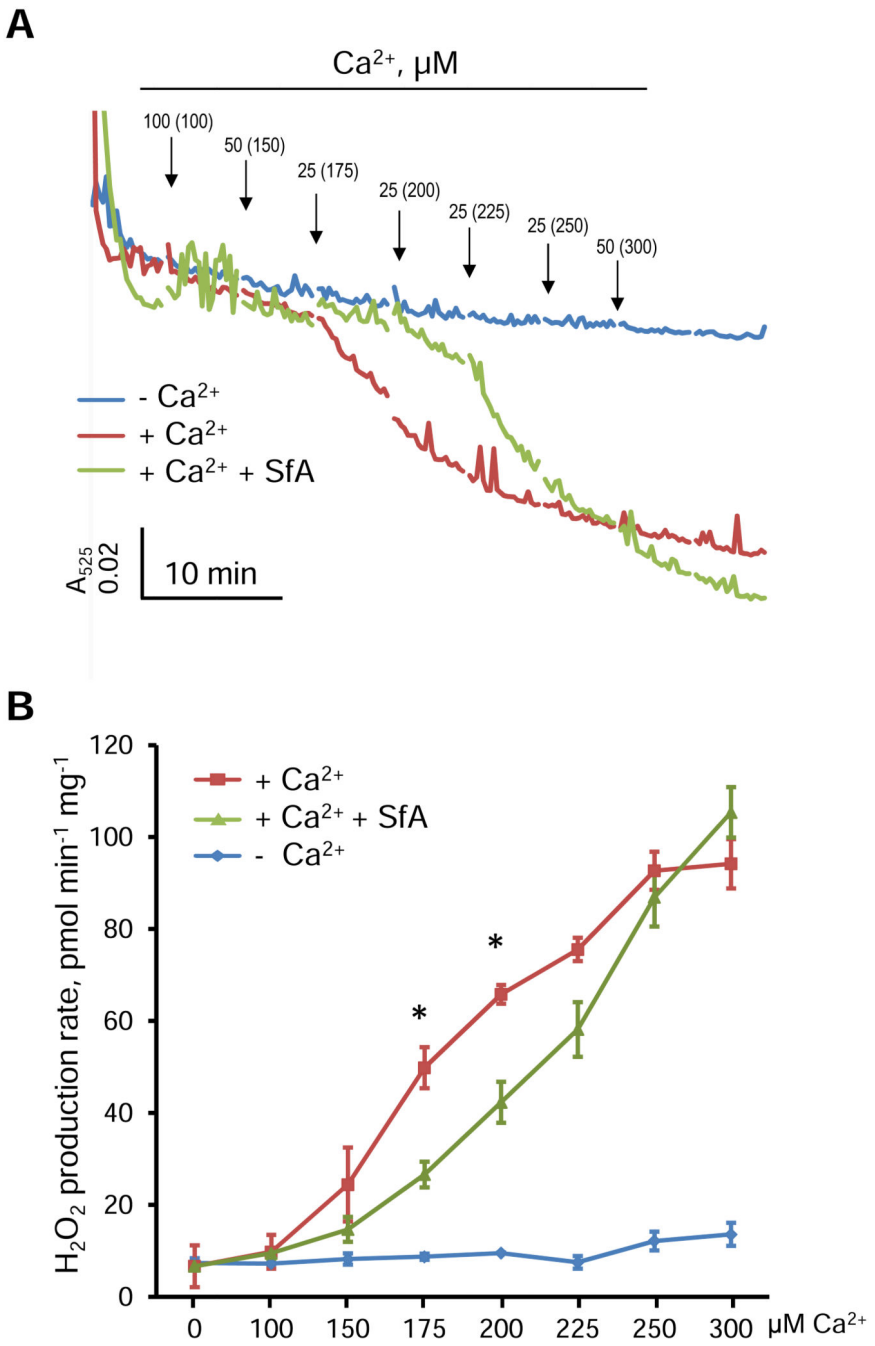

Figure 4.

The effects of SfA on mitochondrial swelling and H_2O_2 production rate in isolated mitochondria. ***A,*** Swelling curves of mitochondria induced by Ca^{2+} in the absence or presence of 0.5 μM SfA. Each arrow indicates the addition of $Ca^{2+}$and final concentrations of Ca^{2+} for each point are given in brackets. Error bars for swelling curves were omitted for better comparison. The representative curves with error bars are shown in Supplementary Figure S2. ***B,*** The effects of Ca^{2+} in the concentration range of 0-300 μM on the H_2O_2

production rate in the absence or presence of 0.5 μM SfA. *P<0.05 vs. +Ca^{2+}+SfA group. Data are shown as means ± SEM (n=6).

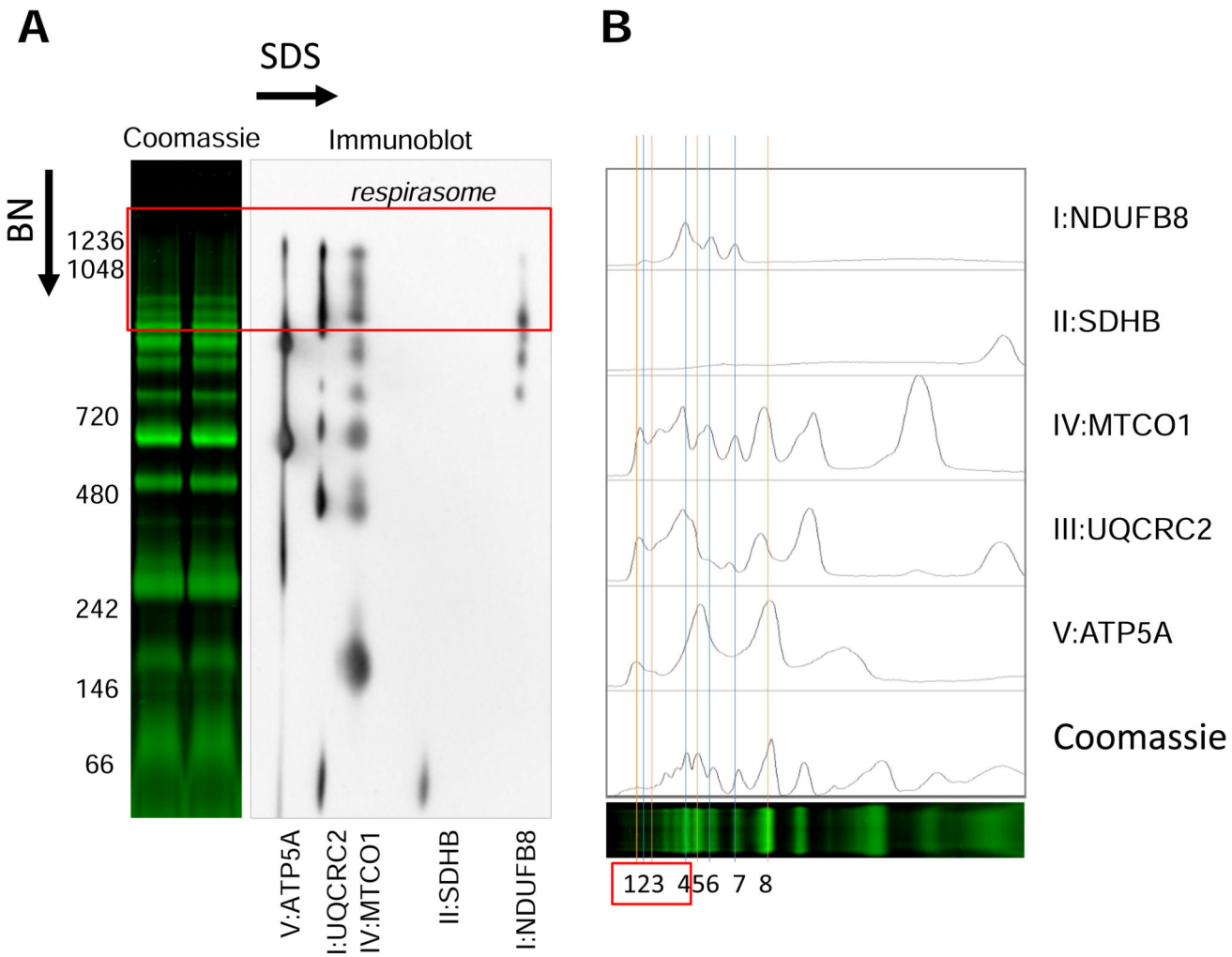

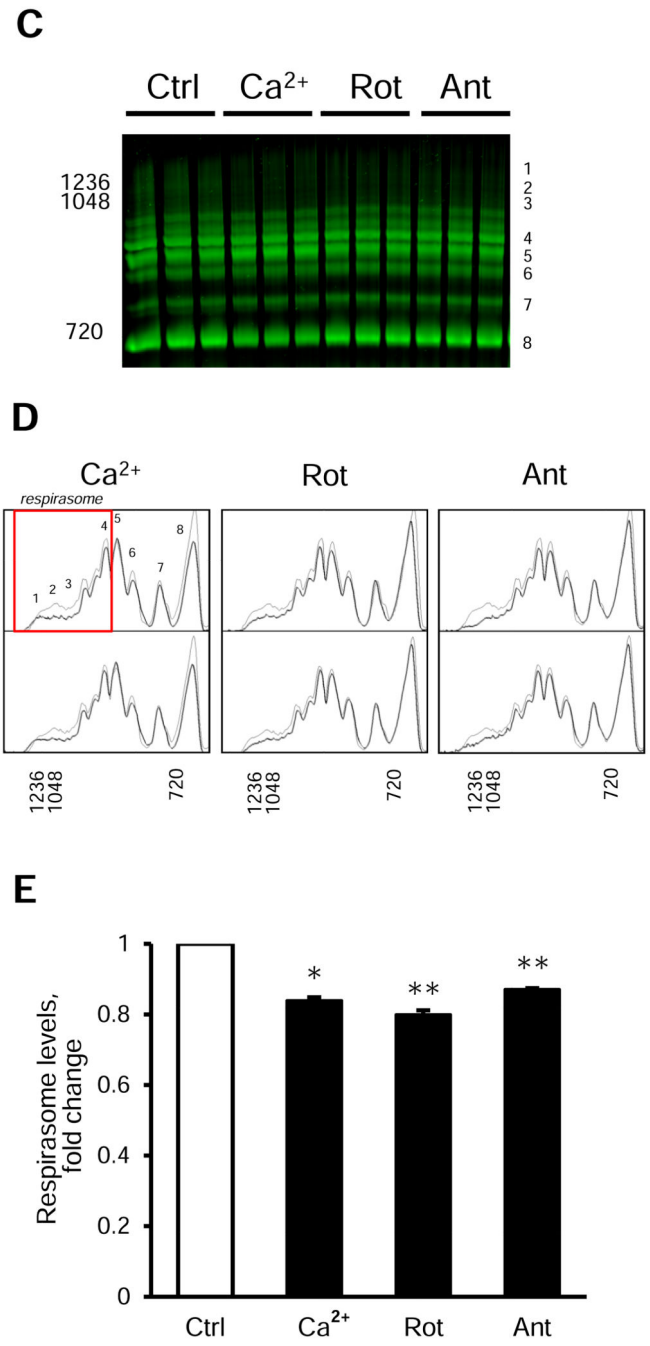

Figure 5.

Analysis and identification of respiratory SCs using the 2D BN/SDS-PAGE and immunoblotting. ***A,*** Identification of bands corresponding to individual ETC complexes I-V after the 2D BN/SDS-PAGE and immunoblotting. ***B***, Histogram analysis of panel ***A***. ***C-E***, Effects of 2 μM rotenone (Rot, complex I inhibitor), 1 μM antimycin A (Ant, complex III inhibitor), and 1 mM Ca^{2+} on the respirasome (SC I_1+III_2+IV_1) level in isolated mitochondria. Representative images of SCs, including the respirasome (*red rectangle*) (***C***), histogram analysis (***D***) of control (*thin lines)* and experimental (*bold lines*) groups, and

quantitative data (***E***) of the respirasome (the sum of peaks 1-4 in ***D***) after BN-PAGE analysis. For 2D BN/SDS-PAGE and immunoblotting, the lanes were cut from native gels after BN-PAGE and immediately incubated with loading buffer (50 mM Tris, pH 8.8, 50 mM DTT, 2% SDS, and 0.01% bromophenol blue) for 5 min. Then, the lanes were loaded into 12% SDS-PAGE gel and sealed with 0.5% agarose. Second-dimension run and subsequent immunoblotting were conducted as per the manufacturer's recommendations (Bio-Rad). ETC complexes I-V were identified using the total OXPHOS Rodent WB Antibody Cocktail (Abcam) as per the manufacturer's recommendations. The cocktail contained antibodies against NDUFB8 (complex I), SDHB (complex II), UQCRC2 (complex III), MTCO1 (complex IV), and ATP5A (complex V). * $P<0.05$, ** $P<0.01$ vs. control (Ctrl). Data are shown as means ± SEM (n=6).